Fat-Specific Sirt6 Ablation Sensitizes Mice to High-Fat Diet–Induced Obesity and Insulin Resistance by Inhibiting Lipolysis

Jiangying Kuang,[1,2] Yuwei Zhang,[3] Qinhui Liu,[2] Jing Shen,[1,2] Shiyun Pu,[1,2] Shihai Cheng,[1,2] Lei Chen,[1,2] Hong Li,[1,2] Tong Wu,[1,2] Rui Li,[1,2] Yanping Li,[1,2] Min Zou,[1] Zhiyong Zhang,[1] Wei Jiang,[4] Guoheng Xu,[5] Aijuan Qu,[6] Wen Xie,[7] and Jinhan He[1,2]

Diabetes 2017;66:1159–1171 | DOI: 10.2337/db16-1225

Sirt6 is an NAD$^+$-dependent deacetylase that is involved in the control of energy metabolism. However, the tissue-specific function of Sirt6 in the adipose tissue remains unknown. In this study, we showed that fat-specific Sirt6 knockout (FKO) sensitized mice to high-fat diet–induced obesity, which was attributed to adipocyte hypertrophy rather than adipocyte hyperplasia. The adipocyte hypertrophy in FKO mice likely resulted from compromised lipolytic activity as an outcome of decreased expression of adipose triglyceride lipase (ATGL), a key lipolytic enzyme. The suppression of ATGL in FKO mice was accounted for by the increased phosphorylation and acetylation of FoxO1, which compromises the transcriptional activity of this positive regulator of ATGL. Fat-specific Sirt6 KO also increased inflammation in the adipose tissue, which may have contributed to insulin resistance in high-fat diet–fed FKO mice. We also observed that in obese patients, the expression of Sirt6 expression is reduced, which is associated with a reduction of ATGL expression. Our results suggest Sirt6 as an attractive therapeutic target for treating obesity and obesity-related metabolic disorders.

Obesity is characterized by excessive triglyceride storage that enlarges adipose tissue. The growth of adipose tissue could result from adipocyte hyperplasia (cell number increase) and/or hypertrophy (cell size increase). Hypertrophy, a result of imbalanced triglyceride synthesis and breakdown, occurs before hyperplasia to meet the need for additional fat storage capacity during the progression of obesity (1,2).

Lipolysis is a process of triglyceride breakdown that liberates glycerol and free fatty acid for other organs to use as energy substrates. Impaired lipolysis results in excess storage of triglycerides that causes adipocyte hypertrophy and obesity (1,3,4). Lipolysis in adipose tissue is tightly regulated by complex regulatory mechanisms involving lipase themselves and hormonal and biochemical signals (1). Lipolysis is stimulated by catecholamines that activate cAMP-dependent protein kinase (PKA) and results in phosphorylation of perilipin 1 (Plin1) and hormone-sensitive lipase (HSL) (1). When phosphorylated, Plin1, which coats the surface of lipid droplets, alleviates the barrier function of this protein and promotes its active participation in the lipolytic process (5). The phosphorylation of HSL causes activation and subsequent translocation of this lipase from the cytosol to lipid droplets (5).

The full lipolytic reaction requires adipose triglyceride lipase (ATGL), which is now considered the rate-limiting lipolytic enzyme (6–9). ATGL catalyzes the initial step,

[1]Department of Pharmacy, State Key Laboratory of Biotherapy, West China Hospital, Sichuan University, Chengdu, Sichuan, China
[2]Laboratory of Clinical Pharmacy and Adverse Drug Reaction, State Key Laboratory of Biotherapy, West China Hospital, Sichuan University, Chengdu, Sichuan, China
[3]Division of Endocrinology and Metabolism, State Key Laboratory of Biotherapy, West China Hospital, Sichuan University, Chengdu, Sichuan, China
[4]Molecular Medicine Research Center, State Key Laboratory of Biotherapy, West China Hospital, Sichuan University, Chengdu, Sichuan, China
[5]Department of Physiology and Pathophysiology, School of Basic Medical Sciences, Peking University, Beijing, China
[6]Department of Physiology and Pathophysiology, School of Basic Medical Sciences, Capital Medical University, Beijing, China
[7]Center of Pharmacogenetics, School of Pharmacy, University of Pittsburgh, Pittsburgh, PA

Corresponding author: Jinhan He, jinhanhe@scu.edu.cn.

Received 11 October 2016 and accepted 16 February 2017.

This article contains Supplementary Data online at http://diabetes.diabetesjournals.org/lookup/suppl/doi:10.2337/db16-1225/-/DC1.

converting triglycerides to diacylglycerols, whereas HSL and other lipase mainly hydrolyzes the diacylglycerols to monoacylglycerol and glycerol. Loss of ATGL reduces lipolysis in adipocyte and was accompanied by increased adipose tissue weight (10,11), whereas its overexpression promotes lipolysis (12). The expression of ATGL is controlled by FoxO1 and peroxisome proliferator–activated receptor γ (PPARγ) as a target gene (9,13). Insulin-inhibited lipolysis is believed to be mediated by suppressing FoxO1 activity and thereby reducing ATGL expression (9).

Sirt6, an NAD^+-dependent protein deacetylase, plays a key role in metabolism. Sirt6-deficient mice show severe hypoglycemia, which causes their premature death within 4 weeks (14). Sirt6 expression is induced in liver by caloric restriction and suppressed in fatty liver disease (15). Hepatic-specific deletion of Sirt6 results in triglyceride accumulation in liver by increasing fatty acid uptake and reducing fatty acid oxidation (16). Whole-body overexpression of Sirt6 was associated with improved blood lipid profiles in mice fed a high-fat diet (HFD) (17). Recent reports indicated a possible function of Sirt6 in adipose tissue. Sirt6 expression was reduced in adipose tissue of *db/db* mice, a model of obesity (18). In contrast, Sirt6 expression was increased in adipose tissue of human subjects with weight loss (19). Although these studies suggested that Sirt6 might play a role in adipose tissue, the exact function and underlying mechanism remains unclear.

In this study, we investigated the function of Sirt6 by using fat-specific Sirt6 knockout (FKO) mice and Sirt6 KO adipocytes. Fat-specific Sirt6 KO promoted HFD-induced obesity because of impaired lipolytic activity. The impaired lipolysis in FKO mice is attributed to reduced expression of ATGL. Mechanistically, Sirt6 deficiency increased the acetylation of FoxO1, promoted FoxO1 nuclear export, and reduced its positive regulation on ATGL. In addition, FKO was associated with increased inflammation in adipose tissue and exacerbated HFD-induced insulin resistance and fatty liver disease. Finally, Sirt6 expression was suppressed in obese patients, which was associated with decreased expression of ATGL. Our results reveal an essential role of Sirt6 in obesity and related metabolic disorders.

RESEARCH DESIGN AND METHODS

Animals, Diet Treatment, and Histology

All animal protocols were reviewed and approved by the Animal Care and Use Committee of Sichuan University. Sirt6 heterozygous mice, adipoq-Cre mice, and $Sirt6^{Loxp/Loxp}$ mice were purchased from The Jackson Laboratory (Bar Harbor, ME). For the HFD-induced obesity model, 6-week-old mice received an HFD (D12492; Research Diets) for 8–12 weeks as indicated. The adipocyte surface areas were quantified as described (20).

Glucose and Insulin Tolerance Tests

Glucose tolerance test (GTT) and insulin tolerance test (ITT) were performed as we previously described (21).

Immunoprecipitation and Western Blot Analysis

For immunoprecipitation, cells were lysed into nondenaturing lysis buffer as described (22). Antibodies are listed in Supplementary Table 1.

Mouse Embryonic Fibroblast Isolation and Differentiation

Embryos were harvested at 12.5 to 13.5 days, and mouse embryonic fibroblasts (MEFs) were plated as monolayer cultures in DMEM with 10% FBS. The MEFs were differentiated into adipocytes as described (23).

Isolation of White Adipose Tissue Explants and Lipolysis Measurement

White adipose tissue (WAT) explants (~20 mg) were isolated from epididymal adipose tissue and washed with PBS three times as previously described (24). Glycerol released from explants into the culture medium was determined as an index of lipolysis (25).

Flow Cytometry

To detect macrophage infiltration, stromal vascular fraction (SVF) was stained with fluorescence-labeled primary antibodies and analyzed by using CytoFlex (Beckman Coulter, Indianapolis, IN).

Human Adipose Tissue Samples

Adipose tissue samples were isolated from freshly excised human abdominal fat tissue from donors who underwent elective operations (e.g., abdominoplasty) at the Department of Surgery, West China Hospital, Sichuan University. The names of the patients were kept anonymous, and all patients used for experiments were without diabetes and aged 28–47 years.

Real-Time PCR and Chromatin Immunoprecipitation Assay

Real-time PCR and chromatin immunoprecipitation (ChIP) assay were performed as described (26,27). Primer sequences are listed in Supplementary Tables 2 and 3.

Statistical Analysis

Statistical significance was determined by Student unpaired two-tailed *t* test or one-way ANOVA multiple-comparison test. A P value <0.05 was considered statistically significant.

RESULTS

Fat-Specific Sirt6 Ablation Sensitizes Mice to HFD-Induced Obesity

To determine the function of Sirt6 in the adipose tissue, we first evaluated whether the adipose expression of Sirt6 could be changed by nutritional challenges such as fasting and overnutrition. Upon 24-h fasting, the adipose expression of Sirt6 was significantly induced (Fig. 1*A*, left panel). In contrast, the adipose expression of Sirt6 was greatly suppressed in HFD-fed mice and *ob/ob* mice (Fig. 1*A*, middle and right panels). Interestingly, the expression of Sirt6 was also suppressed in adipose tissue of aged mice (Supplementary Fig. 1*A*). The expression of Sirt6 seemed to be positively regulated by Sirt1, because overexpression of Sirt1 or

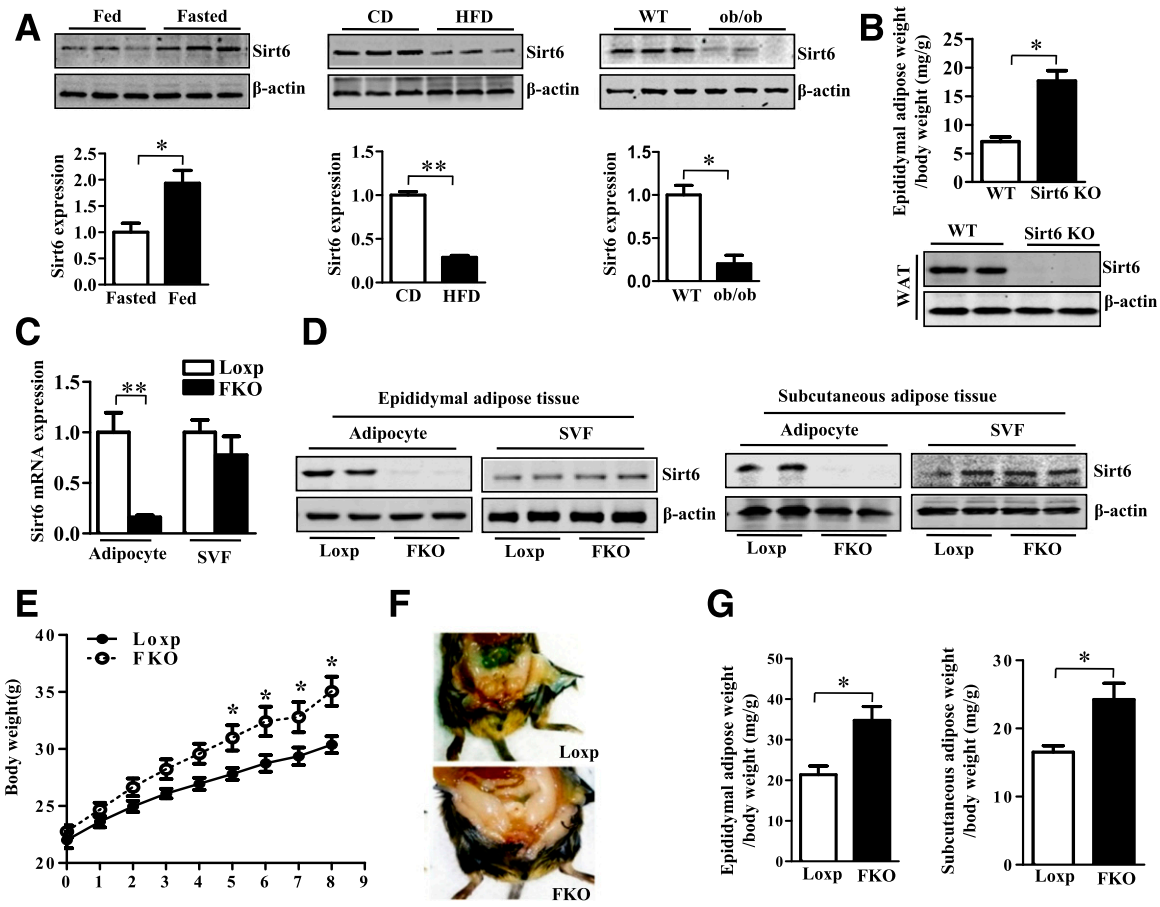

Figure 1—Sirt6 ablation promote obesity. *A*: Sirt6 expression in epididymal adipose tissue from fed and fasted mice (8 weeks old), chow diet (CD)– and HFD-fed mice (16 weeks old), and WT and *ob/ob* mice (14 weeks old). *B*, top: Sirt6 KO mice with 10% glucose feeding for 6 weeks; bottom: Western blot analysis of Sirt6 protein expression in adipose tissue of WT and Sirt6 KO mice. *C*: Real-time PCR analysis of Sirt6 expression in adipocytes and SVF from adipose tissue from Loxp and FKO mice (n = 6). *D*: Western blot analysis of Sirt6 protein expression in adipocytes and SVF of epididymal and subcutaneous adipose tissue from Loxp and FKO mice. *E*: Body weight of Loxp and FKO mice fed with HFD (n = 10). *F:* Representative photographs of Loxp and FKO mice fed with HFD. *G*: The ratio of epididymal and subcutaneous adipose tissue weight to body weight from Loxp and FKO with HFD (n = 15). All data are mean ± SEM. *P < 0.05; **P < 0.01.

activation of Sirt1 by resveratrol increased the expression of Sirt6 in adipocytes (Supplementary Fig. 1*B* and *C*). The dynamics of Sirt6 expression prompted us to explore whether this deacetylase could contribute to energy metabolism in adipose tissue.

Adipose tissue mass was analyzed in whole-body Sirt6 KO mice. Sirt6 KO mice died shortly after weaning because of severe hypoglycemia (14); however, this partial postnatal lethality could be rescued by feeding the mice with 10% glucose-containing water (28). Therefore, we compared adipose tissue weight in Sirt6 KO mice and wild-type (WT) mice fed with water-containing glucose for 6 weeks. Surprisingly, Sirt6 KO mice showed a significant increase in the ratio of WAT weight to body weight (Fig. 1*B*). To determine the role of Sirt6 specifically in the adipose tissue, we generated FKO mice by crossbreeding the floxed Sirt6$^{Loxp/Loxp}$ mice with the adiponectin-derived Cre-transgenic mice (29). The mRNA expression of Sirt6 was decreased by ~80% in the mature adipocytes of epididymal adipose tissue from FKO mice, but not in the SVFs, which are a source of preadipocytes and macrophages (Fig. 1*C*). Consistently, the protein level of Sirt6 was also significantly decreased in mature adipocytes from both epididymal and subcutaneous adipose tissue of FKO mice (Fig. 1*D*). As expected, the expression of Sirt6 was not changed in liver, muscle, or other tissues of FKO mice (Supplementary Fig. 1*D*).

FKO mice were grossly normal and displayed comparable levels of blood glucose under ad libitum and fasting conditions (Supplementary Fig. 2*A* and *B*), which suggests that the hypoglycemia and lethal phenotype observed in Sirt6 KO mice (14) may not be because of the lack of Sirt6 in the adipose tissue. FKO mice on a chow diet showed modestly higher epididymal adipose weight despite having a similar body weight (Supplementary Fig. 2*C* and *D*). When challenged with an HFD, FKO mice gained more body weight than their Loxp counterparts (Fig. 1*E*). Necropsy revealed a significant increase in epididymal and subcutaneous adipose weight in FKO mice (Fig. 1*F* and *G* and

Supplementary Fig. 3*A*). The ambulatory activity and food intake were similar between Loxp and FKO mice (Supplementary Fig. 3*B* and *C*). Together, these data indicate that fat-specific ablation of Sirt6 sensitizes mice to HFD-induced obesity.

Sirt6 Ablation Results in Adipocyte Hypertrophy Without Affecting Adipocyte Differentiation

An increased mass of adipose tissue can result from an induction of adipocyte size, number because of abnormal differentiation, or both (25). To understand the mechanism of increased adiposity seen in FKO mice, we first measured the adipocyte size in adipose tissue of the HFD-fed Loxp and FKO mice. Hematoxylin and eosin (H&E) staining showed that the size of adipocyte was larger in both epididymal and subcutaneous adipose tissue from FKO than Loxp mice (Fig. 2*A* and Supplementary Fig. 3*D*). The increased adipocyte size in FKO adipose tissue was further supported by cell size quantification (Fig. 2*B* and Supplementary Fig. 3*D*). Despite the adipocyte hypertrophy, the expression of adipogenic transcription factors, C/EBPα/β/δ, and PPARγ, was not changed in the FKO mice (Fig. 2*C*, left panel). The expression of markers of adipocyte differentiation such as adipocyte fatty acid–binding protein (Fabp4) and lipoapoprotein lipase (Lpl) were not changed either (Fig. 2*C*, right panel). The mRNA expression of genes involved fatty acid uptake was not changed (Supplementary Fig. 4*A*, left panel). Interestingly, the β-oxidative gene expression in adipose tissue was slightly higher in FKO mice, probably an in vivo compensatory mechanism aimed at restraining excessive body weight gain caused by Sirt6 deletion in fat tissue (Supplementary Fig. 4*A*, right panel).

The effect of Sirt6 ablation on adiposity was also supported by in vitro results. In this experiment, MEFs were isolated from WT and Sirt6 KO embryos and then subjected to in vitro differentiation to adipocytes. During differentiation of WT MEFs, Sirt6 expression was gradually increased, which suggests a role of Sirt6 in lipid metabolism (Fig. 2*D*). The Sirt6 KO MEFs differentiated normally as supported by their comparable gene expression of adipogenic markers, fatty acid uptake, and β-oxidation, except acyl-CoA oxidase (Fig. 2*E* and *F* and Supplementary Fig. 4*B*). Oil Red O staining indicated Sirt6 KO adipocytes showed higher lipid accumulation than WT cells (Fig. 2*G* and *H*). Similarly, Sirt6 overexpression did not affect adipogenic markers, fatty acid uptake, and oxidative gene expression (Fig. 2*I* and *J* and Supplementary Fig. 4*C*). Thus, our in vivo and in vitro results suggested Sirt6 ablation might cause adipocyte hypertrophy because of greater triglyceride accumulation and larger adipocyte size rather than abnormal adipocyte differentiation.

Sirt6 Ablation Inhibits Lipolysis and Suppresses the Expression of ATGL

To determine whether the markedly increased adiposity observed in FKO mice was a result of impaired lipolytic activity, we compared the lipolysis in explants of WAT from HFD-fed Loxp and FKO mice. The basal rate of glycerol release was similar in adipose explants of Loxp and FKO mice, but when treated with isoproterenol (ISO), which stimulates lipolysis by activating the PKA pathway, the lipolytic rate was significantly lower in epididymal adipose explants from FKO than control mice (Fig. 3*A*). The decreased lipolysis was further supported by reduced expression of ATGL and phosphorylation of HSL and Plin1 in FKO mice compared with Loxp mice fed with HFD in both epididymal and subcutaneous adipose tissue (Fig. 3*B* and Supplementary Fig. 5). The decreased expression of ATGL was also observed in both epididymal and subcutaneous adipose tissue of the FKO mice that were maintained on chow diet (Supplementary Figs. 6 and 7).

Because of the heterogeneity of cell populations within adipose explants, we also examined the effect of Sirt6 ablation on lipolysis directly in adipocytes differentiated from MEFs. In agreement with the results from WAT explants, both basal and stimulated lipolysis were significantly decreased in Sirt6 KO adipocytes (Fig. 3*C*). Again, the protein level of ATGL and phosphorylation of HSL and Plin1 were decreased in Sirt6 KO adipocytes (Fig. 3*D* and Supplementary Fig. 8*A*).

We then used the Sirt6 gain-of-function model to further demonstrate the effect of Sirt6 on lipolysis. Under the basal condition, Sirt6 had no effect on lipolysis, which is probably because of a low basal rate of lipolytic activity (Fig. 3*E*). However, when the adipocytes were stimulated with ISO, lipolysis was significantly higher in Sirt6-overexpressing adipocytes than the control adipocytes (Fig. 3*E*). Consistently, the protein level of ATGL and the phosphorylation of HSL and Plin1 were higher in Sirt6-overexpressing adipocytes (Fig. 3*F* and Supplementary Fig. 8*B*). To further confirm that Sirt6 can regulate ATGL expression in vivo, we injected the Sirt6-expressing adenovirus into the adipose tissue of the *ob/ob* mouse with overnutrition. As shown in Supplementary Fig. 9*A* and *B*, the expression of ATGL was greatly suppressed in *ob/ob* mice. In the same Ad-Sirt6–infected adipose tissue, the expression of ATGL was increased, and the size of adipocyte (Supplementary Fig. 9*A* and *B*) was subsequently decreased (Supplementary Fig. 9*C* and *D*). These results together suggested that Sirt6 is both necessary and sufficient to affect lipolysis, which was associated with the regulation of ATGL expression and phosphorylation of HSL and Plin1.

Sirt6 Regulated ATGL Expression by Modulating FoxO1 Acetylation and Subcellular Localization

To understand the mechanism by which Sirt6 regulates the expression of ATGL, we evaluated the localization, expression, and transcriptional activity of FoxO1, a well-known positive transcriptional regulator of ATGL (9). Immunofluorescence staining revealed that Sirt6 KO changed the subcellular localization FoxO1, which is critical for FoxO1 activity (Fig. 4*A*). The results of immunofluorescence were further confirmed by Western blot analysis showing that Sirt6 ablation promoted FoxO1 nuclear export and its cytoplasm accumulation (Fig. 4*B*), suggesting a decrease in

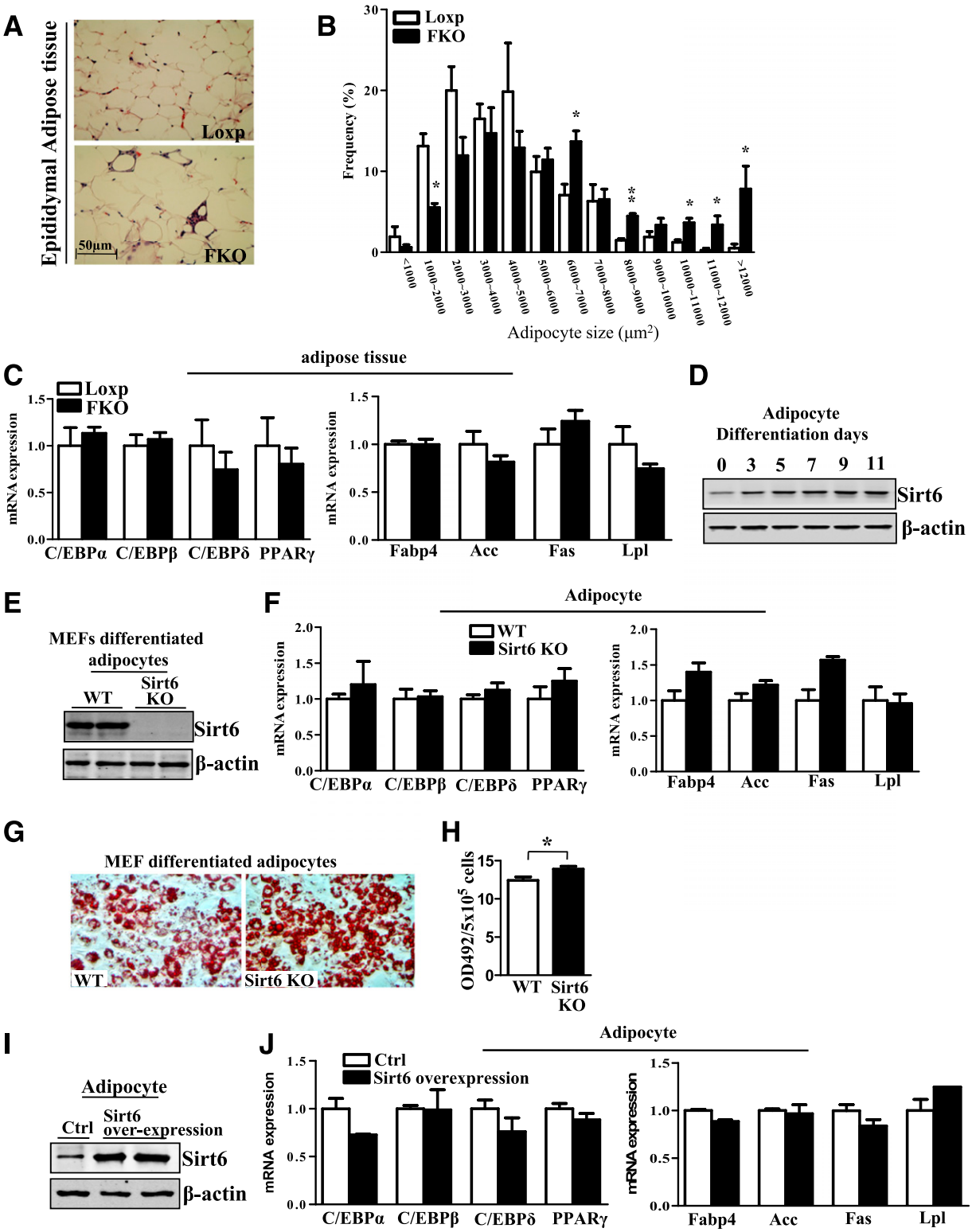

Figure 2—Sirt6 KO causes adipocyte hypertrophy rather than abnormal adipocyte differentiation. *A*: Representative H&E-stained sections of epididymal adipose tissue from Loxp and FKO mice with HFD. *B*: Frequency distribution of adipocyte cell size in epididymal adipose tissue from Loxp and FKO mice with HFD (n = 6). *C*: Real-time PCR analysis of adipogenic gene expression in epididymal adipose tissue from Loxp and FKO mice with HFD (n = 15). *D*: Western blot analysis of Sirt6 expression in differentiated MEF adipocytes from WT mice. Day 0 represents undifferentiated MEF cells. *E* and *F*: MEFs from WT and Sirt6 KO embryos were differentiated for 8 days. Sirt6 expression is confirmed by Western blot analysis, and adipogenic gene expression was profiled. *G* and *H*: Oil Red O staining and quantification of differentiated adipocytes from WT and Sirt6 KO MEF. *I* and *J*: Western blot analysis of Sirt6 expression and real-time PCR analysis of adipogenic gene expression. MEFs from WT embryos treated with Ad-GFP (Ctrl) or Ad-Sirt6 (Sirt6 overexpression) adenovirus and differentiated for 8 days. Each experiment was replicated three times. All data are mean ± SEM. $^*P < 0.05$; $^{**}P < 0.01$.

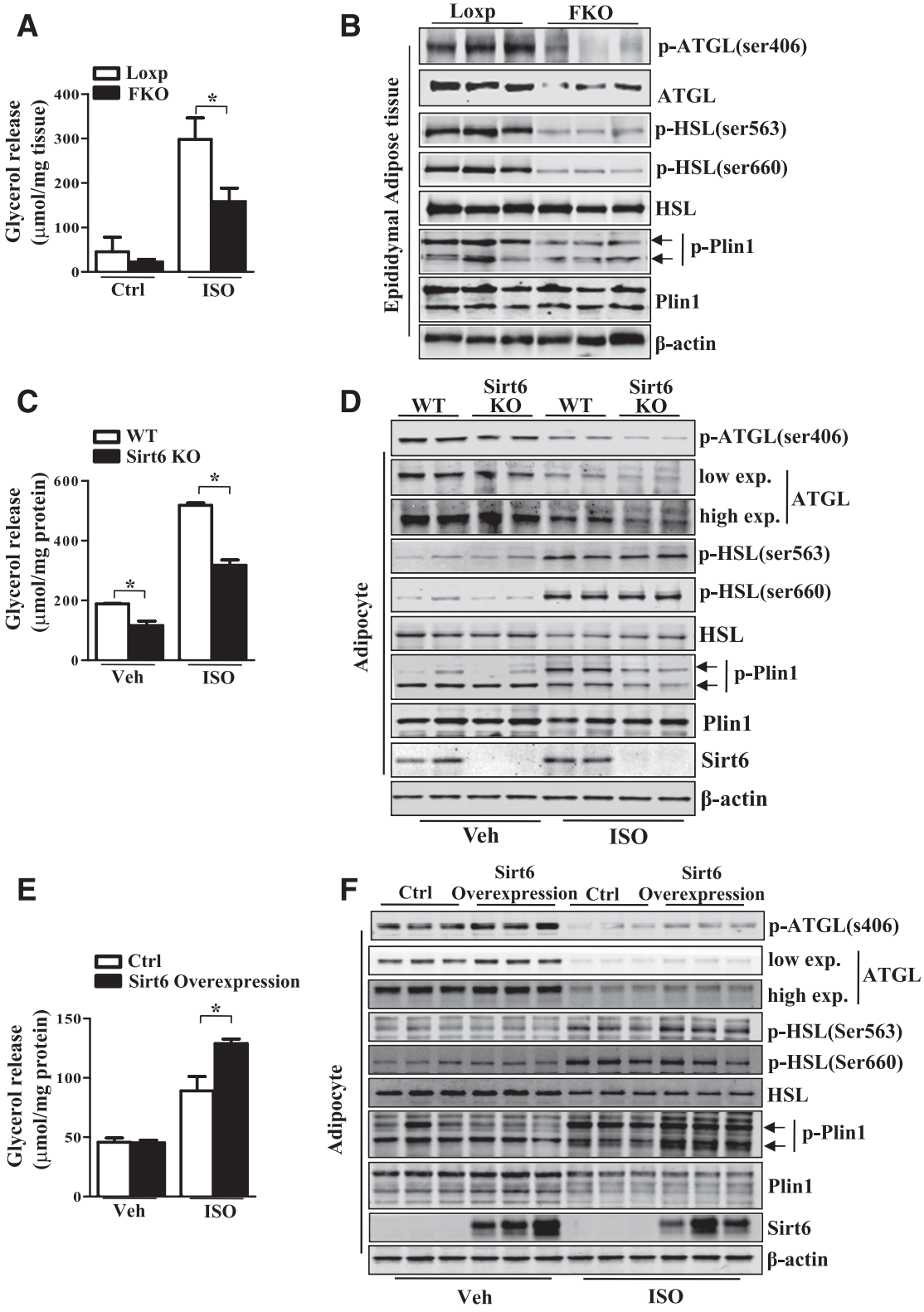

Figure 3—Sirt6 regulates lipolysis in vivo and in vitro. *A*: Basal and stimulated (10 nmol/L ISO) lipolysis, as measured by glycerol release from epididymal adipose tissue explants from 16-week-old Loxp and FKO mice fed with an HFD ($n = 5$). *B*: Western blot analysis of expression of key lipolytic proteins in epididymal adipose tissue from Loxp and FKO mice with HFD. *C*: Basal and stimulated (10 nmol/L ISO) lipolysis in adipocytes differentiated from WT and Sirt6 KO MEFs. *D*: Western blot analysis of protein levels of key lipolytic proteins in adipocytes differentiated from WT and Sirt6 KO MEFs. *E*: Basal and stimulated (10 nmol/L ISO) lipolysis in adipocytes with or without Sirt6 overexpression. *F*: Western blot analysis of protein levels of key lipolytic proteins in adipocytes with or without Sirt6 overexpression. Each experiment was replicated for three times. All data are mean ± SEM. *$P < 0.05$. Ctrl, control; exp, exposure; p, phosphorylated; Veh, vehicle.

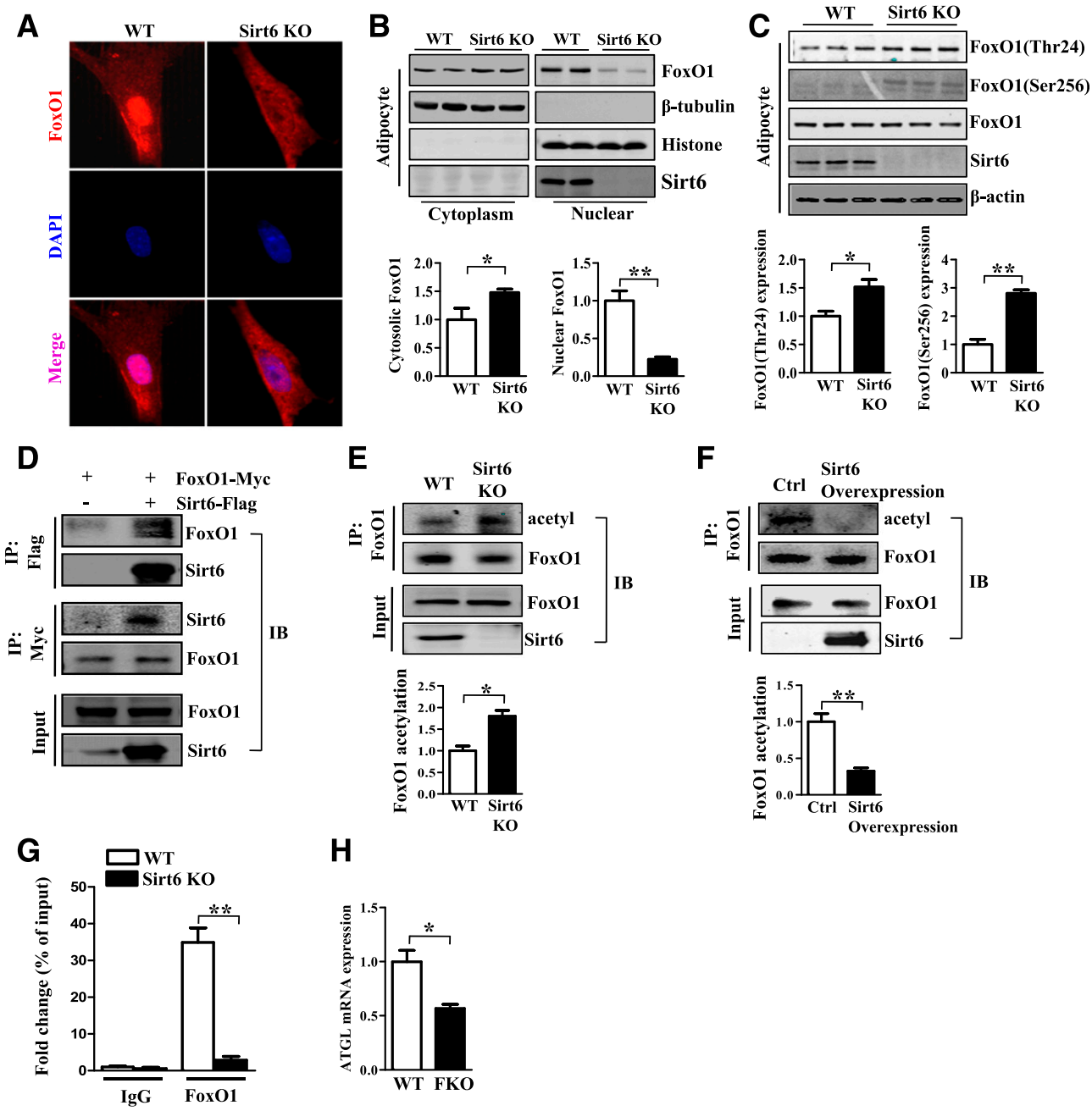

Figure 4—Sirt6 KO inhibited FoxO1 activity by increasing its phosphorylation and acetylation. *A*: Subcellular localization of FoxO1 in WT and Sirt6 KO adipocytes. *B*: Western blot analysis of nuclear and cytoplasm FoxO1 expression in WT and Sirt6 KO MEFs. *C*: Western blot analysis of phosphorylation levels of FoxO1 in adipocytes differentiated from WT and Sirt6 KO MEFs and their quantification in WT and Sirt6 KO MEFs. *D*: The nondenaturing lysates from HEK-293 cells transiently transfected with FoxO1-Myc– and/or Sirt6-Flag–overexpressing constructs were subjected to immunoprecipitation (IP) with anti-Flag or anti-Myc antibody. The precipitated lysates were immunoblotted (IB) with anti-FoxO1 or anti-Sirt6 antibody. Total lysate input was detected by Western blot analysis. *E* and *F*, top: The nondenaturing lysates from WT and Sirt6 KO MEFs or control (Ctrl) and Sirt6 overexpression MEFs were immunoprecipitated with anti-FoxO1. The precipitated lysates were blotted with antiacetylated and anti-FoxO1 antibodies. Total lysate input was detected by Western blot analysis. Bottom panels show the quantification of acetylated protein, normalized to precipitated FoxO1 protein. *G*: ChIP assay of FoxO1 occupancy on the promoter of ATGL in epididymal adipose tissue from WT and Sirt6 KO mice. IgG was a negative control ($n = 3$). *H*: mRNA expression of ATGL in adipose tissue of WT and Sirt6 KO mice ($n = 10$). Each experiment was replicated three times. All data are mean ± SEM. $^*P < 0.05$; $^{**}P < 0.01$.

FoxO1 transcriptional activity. Previous reports showed that the subcellular localization of FoxO1 was regulated by its phosphorylation and acetylation (30,31). Sirt6 ablation increased the phosphorylation of FoxO1 (Fig. 4*C*). Conversely, overexpression of the WT Sirt6, but not the catalytic inactive mutant Sirt6 (H133y), decreased the phosphorylation of FoxO1 (Supplementary Fig. 10*A* and *B*). To understand whether Sirt6 can directly deacetylate FoxO1,

coimmunoprecipitation was performed and showed that Sirt6 physically interacted with FoxO1 in HEK-293 cells (Fig. 4*D*). The interaction between the endogenous Sirt6 and FoxO1 in adipocytes was also confirmed by immunoprecipitation and Western blot analysis (Supplementary Fig. 10*C*). Furthermore, FoxO1 acetylation is increased in the Sirt6 KO cells, whereas its acetylation is decreased in Sirt6-overexpressing cells (Fig. 4*E* and *F*), suggesting Sirt6 directly deacetylates FoxO1. The deacetylation of FoxO1 appeared to be dependent on Sirt6 catalytic activity, because the mutant Sirt6 did not have these effects (Supplementary Fig. 10*D* and *E*).

To further confirm whether the activity of FoxO1 could be affected by its altered phosphorylation and acetylation, we used ChIP assay to measure FoxO1 transcriptional activity on the ATGL gene promoter. The recruitment of FoxO1 to ATGL promoter was significantly decreased in Sirt6 KO adipose tissue (Fig. 4*G*). In agreement with the ChIP results, ATGL natural promoter luciferase reporter assay showed that overexpression of the WT Sirt6, but not the mutant Sirt6, increased the activity of the ATGL reporter gene (Supplementary Fig. 10*F*, left panel). Mutation of the FoxO1 acetylation site lysine (FoxO1 6KQ, which mimics the acetylated state; or FoxO1 6KR, which prevents its acetylation) abolished the regulatory effect of Sirt6 (Supplementary Fig. 10*F*, right panel). Consistently, the ATGL mRNA expression was reduced in Sirt6 KO adipose tissue (Fig. 4*H*). Thus, ablation of Sirt6 promoted FoxO1 cytosolic localization and inhibited its occupancy on the ATGL gene promoter by increasing the phosphorylation and acetylation of FoxO1.

Sirt6 KO Adipocytes Show Increased HFD-Induced Adipose Tissue Inflammation

Obesity is often associated with macrophage infiltration in adipose tissue, which could cause chronic inflammation. Immunochemistry revealed increased staining for $CD11b^+$ and F4/80 in adipose tissue of FKO mice fed an HFD, which indicated macrophage infiltration (Fig. 5*A*). Flow cytometry studies confirmed that $CD11b^+$/F4/80 double-positive adipose tissue macrophages (ATMs) were increased ~60% (Fig. 5*B*, top left panel). ATMs can be further classified into classically activated macrophages (M1), which produce proinflammatory cytokines, and alternatively activated macrophages (M2), which produce anti-inflammatory cytokines. The M1-like polarized $CD11c^+$/$CD11b^+$/F4/80 and triple-positive ATMs were markedly increased in adipose tissue from FKO mice (Fig. 5*B*, top right panel). The M2-like polarized $CD206^+$/$CD11b^+$/F4/80 triple-positive ATMs were not changed (Fig. 5*B*, bottom left panel). As a result, the ratio of M1/M2 was significantly higher in adipose tissue of FKO mice (Fig. 5*B*, bottom right panel). Consistent with these results, mRNA expression of macrophage marker and inflammatory genes such as $CD11b^+$, Cxcl2, CD68, tumor necrosis factor-α (TNF-α), Mcp-1, and interleukin-6 (IL-6) was induced in FKO adipose tissue (Fig. 5*C* and *D*). Sirt6 KO also substantially increased the expression of inflammatory Mcp-1, IL-6, and TNF-α in the in vitro–differentiated adipocytes (Fig. 5*E*). Previous studies showed that c-Jun N-terminal kinase (JNK) was required for proinflammatory macrophage polarization in adipose tissue (32). The JNK was activated in adipose tissue of FKO mice (Fig. 5*F*) and in the Sirt6 KO adipocytes (Fig. 5*G*). ChIP assay also showed Sirt6 ablation increased the occupancy of c-Jun, downstream of JNK, on the gene promoters of IL-6 and Mcp-1, two proinflammatory genes that were dramatically increased in the Sirt6 knockout adipose tissue (Fig. 5*H*). Thus, Sirt6 deficiency may have increased inflammation in adipose tissue of mice.

Fat-Specific Ablation of Sirt6 Promotes HFD-Induced Insulin Resistance

The increased adiposity and inflammation in FKO mice suggested that FKO mice might have compromised glucose metabolism and insulin sensitivity. FKO mice on a chow diet showed a compromised ITT, whereas GTT was similar between the Loxp and FKO mice (Supplementary Fig. 11). When fed with an HFD, the FKO mice showed worse performance in both the GTT and ITT (Fig. 6*A* and *B*). In understanding the mechanism by which Sirt6 ablation exacerbates insulin resistance, we assessed the insulin signaling in the liver, WAT, and skeletal muscle. Insulin-induced phosphorylation of AKT was specifically attenuated in the adipose tissue (Fig. 6*C*), but not in the liver or skeletal muscle of FKO mice (Supplementary Fig. 12), which suggests tissue-specific impairment of insulin sensitivity. Serum chemistry also supported the impaired insulin sensitivity in the HFD-fed FKO mice, including an increase in serum levels of leptin and decrease in serum adiponectin level (Fig. 6*D*).

Hepatic steatosis is associated with obesity and insulin resistance. Oil Red O staining showed increased lipid accumulation in the liver of FKO mice (Fig. 6*E*). Lipid analysis showed that hepatic triglyceride and cholesterol levels were significantly increased in FKO mice (Fig. 6*F*). The mRNA levels of sterol regulatory element–binding protein-1c (Srebp-1c), fatty acid transport protein 1 (Fatp1), Fatp5, and Cd36 were induced in the liver of FKO mice (Fig. 6*G*), but the expression of fatty acid β-oxidative genes was not changed (Supplementary Fig. 13*A*–*C*). Together, the increased hepatic steatosis in FKO mice fed an HFD could be partially explained by increased fatty acid uptake and lipogenesis. The serum lipid profiles were similar between Loxp and FKO mice, except that the serum FFA and triglyceride levels were lower in HFD-fed FKO mice (Supplementary Fig. 13*D*).

Reduced Sirt6 and ATGL Expression in Obese Subjects

Finally, we want to know whether the expression of Sirt6 is changed in adipose tissue of obese patients. Compared with nonobese subjects whose average BMI is 24, the expression of Sirt6 was significantly suppressed in adipose tissue of obese patients whose BMI is >27 (Fig. 7*A* and *B*). The obese subjects also showed a parallel decrease in ATGL expression (Fig. 7*A* and *B*), consistent with the observations in the FKO mice. The expression of ATGL is well correlated with Sirt6 expression in these

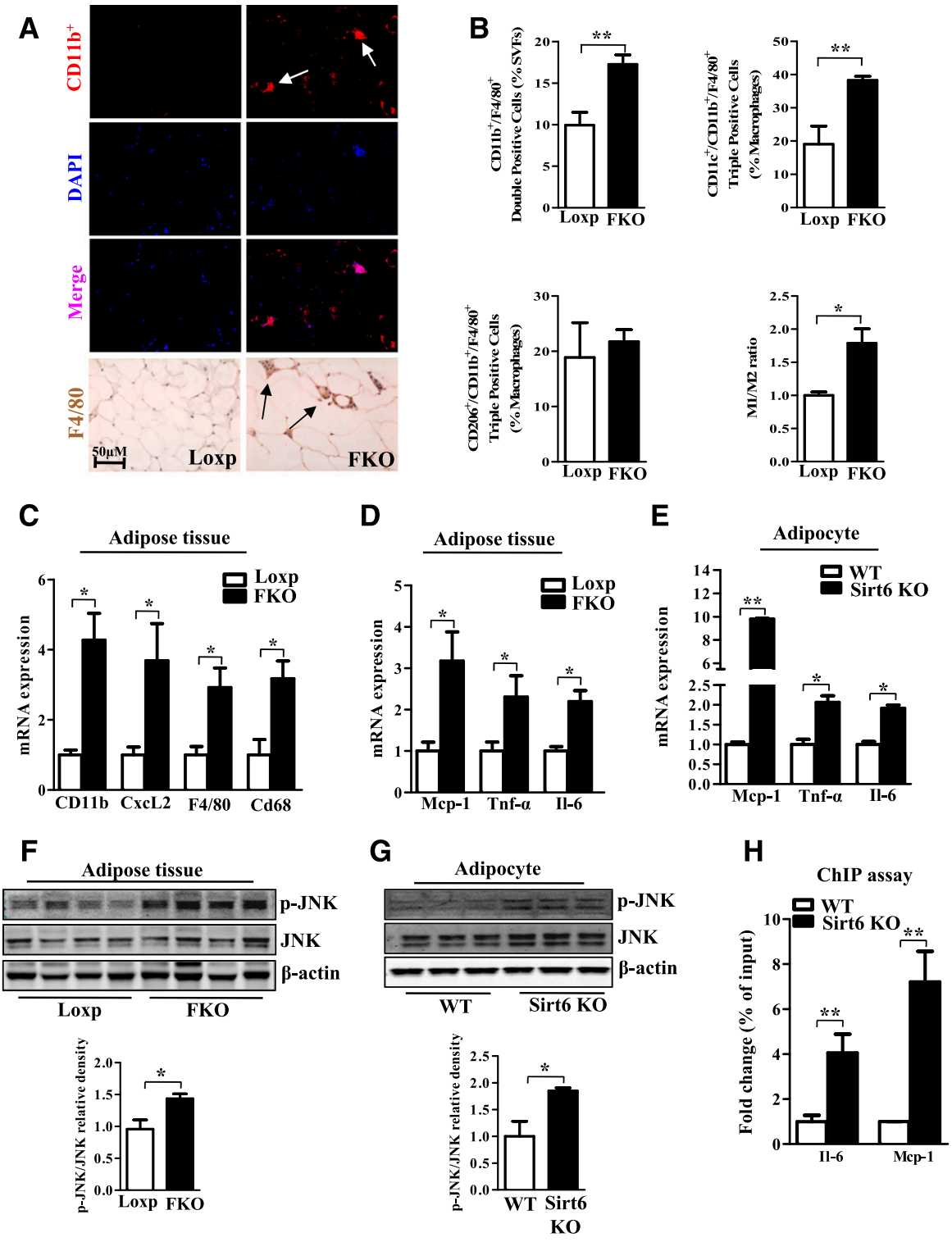

Figure 5—Fat-specific ablation of Sirt6 promotes adipose inflammation. *A*, top panels: Immunofluorescence staining of macrophage markers in adipose tissue. Arrows indicate macrophage infiltration (n = 5). Bottom panels: Immunohistochemical staining of macrophage markers in adipose tissue. Arrows indicate macrophage infiltration. *B*: Flow cytometry analysis of macrophages in epididymal adipose tissue from Loxp and FKO mice with HFD. Top left: $CD11b^+/F4/80$ double-positive indicated the macrophages; top right: $CD11c^+/CD11b^+/F4/80$ triple-positive indicated the M1 macrophages; bottom left: $CD206^+/CD11b^+/F4/80$ triple-positive indicated the M2 macrophages; bottom right: the ratio of M1 to M2 (n = 5). *C*: mRNA expression of macrophage markers in epididymal adipose tissue from control and FKO mice with HFD (n = 10). *D*: Inflammatory cytokine expression in epididymal adipose tissue from control and FKO mice with HFD (n = 10). *E*: Inflammatory cytokine expression in WT and Sirt6 KO adipocytes. *F* and *G*, top panels: Western blot analysis of JNK phosphorylation in adipose tissue from loxp and FKO mice or WT and Sirt6 KO adipocytes. Bottom panels: The quantification of JNK phosphorylation (p), normalized to total JNK. All data are mean ± SEM. *H*: ChIP assay of c-Jun occupancy onto the promoters of IL-6 and Mcp-1 in epididymal adipose tissue from WT and Sirt6 KO mice. Each experiment was replicated three times. All data are mean ± SEM. *P < 0.05; ** P < 0.01.

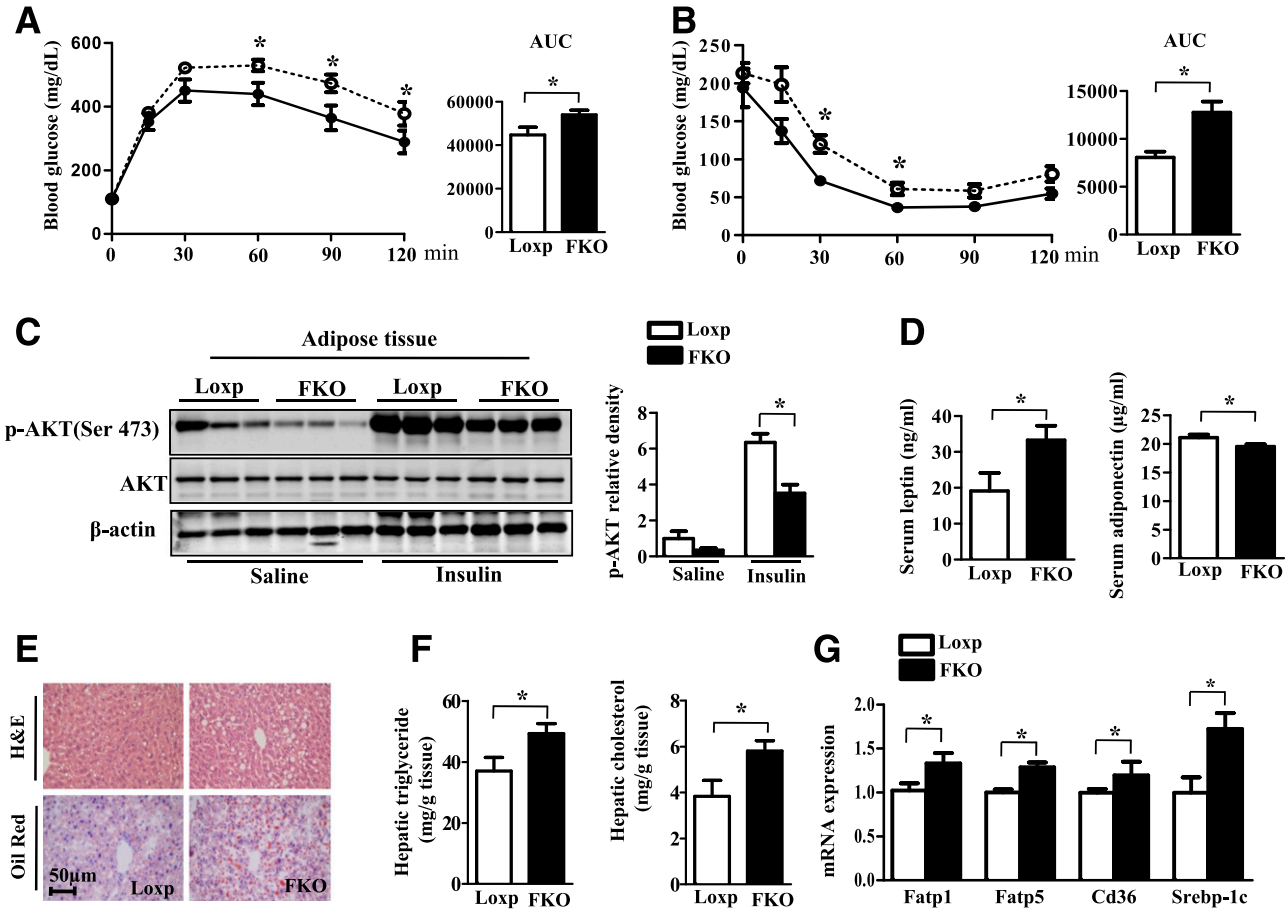

Figure 6—Fat-specific ablation of Sirt6 promotes HFD-induced insulin resistance and hepatic steatosis. GTT (*A*) and ITT (*B*) in Loxp and FKO mice with HFD (n = 15). Left panels: HFD-fed mice were injected with glucose (2 g/kg) or insulin (1 U/kg), and blood glucose was measured at indicated time points by a glucose meter. Right panels: Area under the curve (AUC). *C*: Western blot analysis of AKT phosphorylation in adipose tissue of Loxp and FKO mice with HFD. *D*: Serum leptin and adiponectin levels in overnight-fasted Loxp and FKO mice with HFD. *E*: Representative images of H&E- and Oil Red O–stained sections of liver tissue from Loxp and FKO mice with HFD. *F*: Levels of hepatic triglycerides and cholesterol in liver of Loxp and FKO mice with HFD (n = 8). *G*: Real-time PCR analysis of mRNA levels of hepatic lipogenesis genes from Loxp and FKO mice with HFD. Each experiment was replicated three times. All data are mean ± SEM. *$P < 0.05$. p, phosphorylated.

individuals (Fig. 7*C*). Together, these results indicated that Sirt6 might have a regulatory role of Sirt6 in ATGL expression and obesity in humans.

DISCUSSION

In this study, we found that Sirt6 ablation increased diet induced-obesity through adipocyte hypertrophy rather than abnormal adipocyte differentiation. Adipocyte hypertrophy might be attributed to the impaired lipolytic activity in FKO mice, which causes fat storage synthesis to exceed lipolysis, resulting in obesity. Indeed, a defect in lipolysis has been associated with obesity (25,33). Lipolytic activity was reduced in adipocytes from obese people as compared with nonobese control subjects on stimulation (25,33,34). Lipolytic activity is stimulated acutely during fasting by ISO-stimulated β-adrenergic signaling, leading to PKA phosphorylation of perilipin and HSL (35,36). We found that Sirt6 deficiency decreased the phosphorylation of Plin1 and HSL, with no change in Plin1 and HSL protein expression. Future studies are needed to determine the mechanism by which Sirt6 ablation decreases the phosphorylation level of Plin1 and HSL.

ATGL is the key lipase that hydrolyzes triglycerides into diglycerides, which are further catalyzed by HSL into monoglycerides and glycerols (6). We found ATGL expression is significantly suppressed in adipose tissue of FKO mice. Our results are consistent with a previous report that ATGL ablation was sufficient to compromise lipolysis (10). The downregulation of ATGL may result from the increased phosphorylation and acetylation of FoxO1. ATGL is a direct target of FoxO1 (9). Insulin, an antilipolytic hormone, inhibits the expression of ATGL in adipocytes by increasing FoxO1 phosphorylation, thereby promoting its nuclear exclusion and decreasing its transcriptional activity (9,31). Recent studies also suggested that FoxO1 activity is inactivated with its acetylation during nutrient excess (37). Sirt6 physically interacted with FoxO1, and Sirt6 KO increased the acetylation of FoxO1. Functional

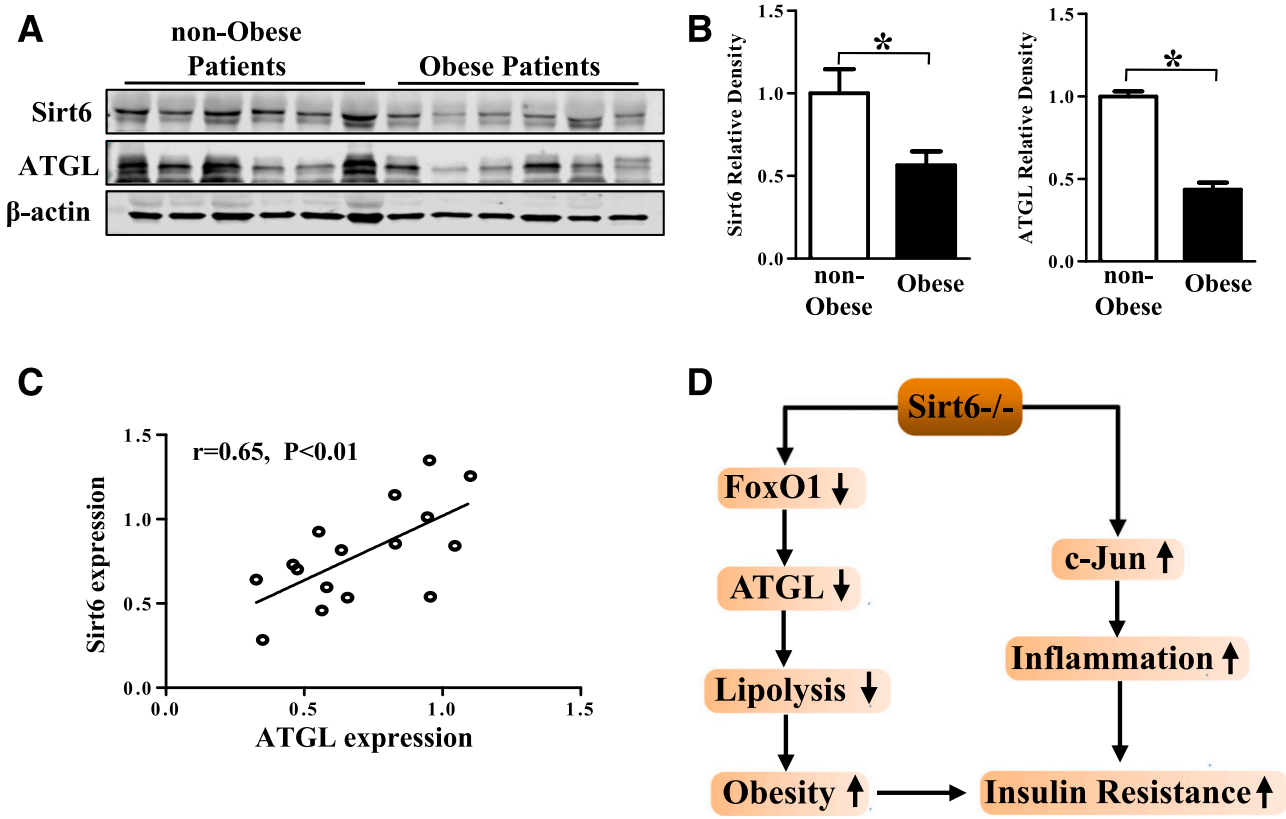

Figure 7—Reduced Sirt6 and ATGL expression in obese patients. Western blot analysis of ATGL and Sirt6 expression (*A* and *B*) and correlation of ATGL and Sirt6 expression (*C*) in adipose tissue of normal and obese patients (n = 6). *D*: Summary of the Sirt6 functions in adipose tissue. Sirt6 deficiency results in decreased FoxO1 activity and lower ATGL expression. Subsequently, lower expression of ATGL reduced lipolysis and causes obesity. Sirt6 deficiency also activated c-Jun and elevated inflammation in the adipose tissue. The obesity and inflammation coordinate to promote insulin resistance. All data are mean ± SEM. *$P < 0.05$.

analysis revealed that Sirt6 KO decreased FoxO1 transcriptional activity in adipocytes. Together, our results provide a plausible mechanism for Sirt6-modulated ATGL expression by regulating FoxO1 activity. The expression of ATGL is also subjected to the regulation by PPARγ (9,13,38). However, we found the expression of PPARγ and its target genes was largely unchanged.

Similar to rodents, we found the expression of Sirt6 is also suppressed by obesity in humans. The suppressed expression of Sirt6 may explain the lower level of ATGL in obesity, which has been observed in other studies (39). The expression of Sirt6 is well correlated with ATGL expression in obese subjects. It is tempting to speculate that Sirt6 might be a therapeutic target for obesity.

Chronic inflammation is an important factor in obesity and contributes to insulin resistance and type 2 diabetes (40). Sirt6 overexpression attenuates nuclear factor-κB activity (41). Conversely, Sirt6 deficiency triggers inflammation by increasing hypoxia-induced factor-1α activity (42). We found that Sirt6 KO promoted inflammatory gene expression in vivo and in vitro. Mcp-1 was greatly induced in adipose tissue of FKO mice and Sirt6 KO adipocytes. Mcp-1 can directly trigger the recruitment of macrophages to adipose tissue, and these macrophages may in turn secrete various cytokines and chemokines that further induce a local inflammatory response (43). Indeed, M1 macrophage infiltration was increased in adipose tissue of FKO mice. In addition, the ratio of M1/M2 was elevated. Our results suggested that the increased inflammatory gene expression might be a result of increased occupancy of c-JNK onto the promoter of inflammatory genes. JNK, a signal that is associated with the inflammation response, is also activated in Sirt6 KO adipose tissue and adipocytes.

The insulin resistance seen in FKO mice likely resulted from combined effects of obesity and inflammation. The reduced lipolysis of FKO adipocytes leads to marked hypertrophy of these cells. These hypertrophic adipocytes may have a compromised response to insulin. The increased adipose inflammation could promote insulin resistance in FKO mice. Sirt6 KO in adipose tissue also sensitized mice to HFD-induced hepatic steatosis, which was associated with increased expression of genes involved in fatty acid uptake and lipogenesis. The fatty acid transporters such as Fatp1, Fatp5, and Cd36 were higher in the liver of the FKO mice. The expression of the lipogenic gene Srebp-1c in the liver was also increased. Therefore, we cannot exclude the

possibility that the fatty liver in FKO mice might be a secondary effect of obesity because of the inability for the animals to store excess energy within the adipose tissues, so the excess lipids are being ectopically deposited in the liver.

In summary, we show that adipose Sirt6 level is decreased in obesity. Fat-specific Sirt6 KO promoted HFD-induced obesity by inhibiting the lipolytic activity. Mechanistically, the lowered lipolysis in FKO mice was caused by reduced lipolytic activity because of impaired ATGL expression. Sirt6 KO increased phosphorylation and acetylation of FoxO1, thereby decreasing its transcriptional activity on ATGL. Our results suggest Sirt6 as an attractive therapeutic target for treating obesity and obesity-related metabolic disorders.

Acknowledgments. The authors thank Dr. Konstantin V. Kandror (Boston University School of Medicine, Boston, MA) for the ATGL promoter reporter.

Funding. This work was supported by the National Natural Science Foundation of China (81471068, 81270926, 81370521, and 81320157), Distinguished Young Scientists of Sichuan Province (2014JQ0034), and the Young Scientist Fellowship of Sichuan University (2013SCU04A17).

Duality of Interest. No potential conflicts of interest relevant to this article were reported.

Author Contributions. J.K. designed and performed experiments and wrote the manuscript. Y.Z., Q.L., J.S., S.P., S.C., L.C., H.L., T.W., R.L., Y.L., and M.Z. helped with experiments. Z.Z., W.J., G.X., A.Q., and W.X. contributed to the discussion and review of the manuscript. J.H. obtained funding, designed experiments, and wrote the manuscript. J.K. and J.H. are the guarantors of this work and, as such, had full access to all the data in the study and take responsibility for the integrity of the data and the accuracy of the data analysis.

References

1. Duncan RE, Ahmadian M, Jaworski K, Sarkadi-Nagy E, Sul HS. Regulation of lipolysis in adipocytes. Annu Rev Nutr 2007;27:79–101
2. Faust IM, Johnson PR, Stern JS, Hirsch J. Diet-induced adipocyte number increase in adult rats: a new model of obesity. Am J Physiol 1978;235:E279–E286
3. Langin D, Dicker A, Tavernier G, et al. Adipocyte lipases and defect of lipolysis in human obesity. Diabetes 2005;54:3190–3197
4. Osuga J, Ishibashi S, Oka T, et al. Targeted disruption of hormone-sensitive lipase results in male sterility and adipocyte hypertrophy, but not in obesity. Proc Natl Acad Sci U S A 2000;97:787–792
5. Zechner R, Zimmermann R, Eichmann TO, et al. Fat signals–lipases and lipolysis in lipid metabolism and signaling. Cell Metab 2012;15:279–291
6. Zimmermann R, Strauss JG, Haemmerle G, et al. Fat mobilization in adipose tissue is promoted by adipose triglyceride lipase. Science 2004;306:1383–1386
7. Grönke S, Mildner A, Fellert S, et al. Brummer lipase is an evolutionary conserved fat storage regulator in Drosophila. Cell Metab 2005;1:323–330
8. Kurat CF, Natter K, Petschnigg J, et al. Obese yeast: triglyceride lipolysis is functionally conserved from mammals to yeast. J Biol Chem 2006;281:491–500
9. Chakrabarti P, Kandror KV. FoxO1 controls insulin-dependent adipose triglyceride lipase (ATGL) expression and lipolysis in adipocytes. J Biol Chem 2009;284:13296–13300
10. Haemmerle G, Lass A, Zimmermann R, et al. Defective lipolysis and altered energy metabolism in mice lacking adipose triglyceride lipase. Science 2006;312:734–737
11. Ahmadian M, Abbott MJ, Tang T, et al. Desnutrin/ATGL is regulated by AMPK and is required for a brown adipose phenotype. Cell Metab 2011;13:739–748
12. Ahmadian M, Duncan RE, Varady KA, et al. Adipose overexpression of desnutrin promotes fatty acid use and attenuates diet-induced obesity. Diabetes 2009;58:855–866
13. Kershaw EE, Schupp M, Guan HP, Gardner NP, Lazar MA, Flier JS. PPARgamma regulates adipose triglyceride lipase in adipocytes in vitro and in vivo. Am J Physiol Endocrinol Metab 2007;293:E1736–E1745
14. Mostoslavsky R, Chua KF, Lombard DB, et al. Genomic instability and aging-like phenotype in the absence of mammalian SIRT6. Cell 2006;124:315–329
15. Kanfi Y, Shalman R, Peshti V, et al. Regulation of SIRT6 protein levels by nutrient availability. FEBS Lett 2008;582:543–548
16. Kim HS, Xiao C, Wang RH, et al. Hepatic-specific disruption of SIRT6 in mice results in fatty liver formation due to enhanced glycolysis and triglyceride synthesis. Cell Metab 2010;12:224–236
17. Kanfi Y, Peshti V, Gil R, et al. SIRT6 protects against pathological damage caused by diet-induced obesity. Aging Cell 2010;9:162–173
18. Dominy JE Jr, Lee Y, Jedrychowski MP, et al. The deacetylase Sirt6 activates the acetyltransferase GCN5 and suppresses hepatic gluconeogenesis. Mol Cell 2012;48:900–913
19. Moschen AR, Wieser V, Gerner RR, et al. Adipose tissue and liver expression of SIRT1, 3, and 6 increase after extensive weight loss in morbid obesity. J Hepatol 2013;59:1315–1322
20. Nguyen A, Tao H, Metrione M, Hajri T. Very low density lipoprotein receptor (VLDLR) expression is a determinant factor in adipose tissue inflammation and adipocyte-macrophage interaction. J Biol Chem 2014;289:1688–1703
21. He J, Gao J, Xu M, et al. PXR ablation alleviates diet-induced and genetic obesity and insulin resistance in mice. Diabetes 2013;62:1876–1887
22. Jiang H, Khan S, Wang Y, et al. SIRT6 regulates TNF-α secretion through hydrolysis of long-chain fatty acyl lysine. Nature 2013;496:110–113
23. Van Meter M, Kashyap M, Rezazadeh S, et al. SIRT6 represses LINE1 retrotransposons by ribosylating KAP1 but this repression fails with stress and age. Nat Commun 2014;5:5011
24. He J, Xu C, Kuang J, et al. Thiazolidinediones attenuate lipolysis and ameliorate dexamethasone-induced insulin resistance. Metabolism 2015;64:826–836
25. Jaworski K, Ahmadian M, Duncan RE, et al. AdPLA ablation increases lipolysis and prevents obesity induced by high-fat feeding or leptin deficiency. Nat Med 2009;15:159–168
26. Pu S, Ren L, Liu Q, et al. Loss of 5-lipoxygenase activity protects mice against paracetamol-induced liver toxicity. Br J Pharmacol 2016;173:66–76
27. He J, Nishida S, Xu M, Makishima M, Xie W. PXR prevents cholesterol gallstone disease by regulating biosynthesis and transport of bile salts. Gastroenterology 2011;140:2095–2106
28. Xiao C, Kim HS, Lahusen T, et al. SIRT6 deficiency results in severe hypoglycemia by enhancing both basal and insulin-stimulated glucose uptake in mice. J Biol Chem 2010;285:36776–36784
29. Eguchi J, Wang X, Yu S, et al. Transcriptional control of adipose lipid handling by IRF4. Cell Metab 2011;13:249–259
30. Qiang L, Banks AS, Accili D. Uncoupling of acetylation from phosphorylation regulates FoxO1 function independent of its subcellular localization. J Biol Chem 2010;285:27396–27401
31. Matsuzaki H, Daitoku H, Hatta M, Aoyama H, Yoshimochi K, Fukamizu A. Acetylation of Foxo1 alters its DNA-binding ability and sensitivity to phosphorylation. Proc Natl Acad Sci U S A 2005;102:11278–11283
32. Kwok KH, Cheng KK, Hoo RL, Ye D, Xu A, Lam KS. Adipose-specific inactivation of JNK alleviates atherosclerosis in apoE-deficient mice. Clin Sci (Lond) 2016;130:2087–2100
33. Liew CW, Boucher J, Cheong JK, et al. Ablation of TRIP-Br2, a regulator of fat lipolysis, thermogenesis and oxidative metabolism, prevents diet-induced obesity and insulin resistance. Nat Med 2013;19:217–226
34. Large V, Reynisdottir S, Langin D, et al. Decreased expression and function of adipocyte hormone-sensitive lipase in subcutaneous fat cells of obese subjects. J Lipid Res 1999;40:2059–2066
35. Carmen GY, Víctor SM. Signalling mechanisms regulating lipolysis. Cell Signal 2006;18:401–408

36. Jocken JW, Blaak EE. Catecholamine-induced lipolysis in adipose tissue and skeletal muscle in obesity. Physiol Behav 2008;94:219–230
37. Banks AS, Kim-Muller JY, Mastracci TL, et al. Dissociation of the glucose and lipid regulatory functions of FoxO1 by targeted knockin of acetylation-defective alleles in mice. Cell Metab 2011;14:587–597
38. Festuccia WT, Laplante M, Berthiaume M, Gélinas Y, Deshaies Y. PPARgamma agonism increases rat adipose tissue lipolysis, expression of glyceride lipases, and the response of lipolysis to hormonal control. Diabetologia 2006;49:2427–2436
39. Steinberg GR, Kemp BE, Watt MJ. Adipocyte triglyceride lipase expression in human obesity. Am J Physiol Endocrinol Metab 2007;293:E958–E964
40. Glass CK, Olefsky JM. Inflammation and lipid signaling in the etiology of insulin resistance. Cell Metab 2012;15:635–645
41. Kawahara TL, Michishita E, Adler AS, et al. SIRT6 links histone H3 lysine 9 deacetylation to NF-kappaB-dependent gene expression and organismal life span. Cell 2009;136:62–74
42. Zhong L, D'Urso A, Toiber D, et al. The histone deacetylase Sirt6 regulates glucose homeostasis via Hif1alpha. Cell 2010;140:280–293
43. Kanda H, Tateya S, Tamori Y, et al. MCP-1 contributes to macrophage infiltration into adipose tissue, insulin resistance, and hepatic steatosis in obesity. J Clin Invest 2006;116:1494–1505